Mathematical Biosciences and Engineering

MBE, 16(6): 6587–6601.
DOI: 10.3934/mbe.2019328
Received: 28 January 2019
Accepted: 28 June 2019
Published: 16 July 2019

http://www.aimspress.com/journal/MBE

Research article

Impact of cross-correlated sine-Wiener noises in the gene transcriptional regulatory system

Guanghui Cheng[1], Yuangen Yao[2], Rong Gui[2,*] and Ming Yi[3,*]

[1] Department of Electrical and Electronic Engineering, Wuhan Polytechnic University, Wuhan, P.R. China
[2] Department of Physics, College of Science, Huazhong Agricultural University, Wuhan, P.R. China
[3] School of Mathematics and Physics, China University of Geosciences, Wuhan, P.R. China

* **Correspondence:** Email: grace@mail.hzau.edu.cn, mingyi@cug.edu.cn.

Abstract: We studied fluctuation-induced switching processes in the gene transcriptional regulatory system under cross-correlated sine-Wiener (CCSW) noises. It is numerically demonstrated that the increase of the multiplicative noise intensity A and cross-correlation time τ in CCSW noises can reduce the concentration of the TF-A monomer and switch to an "off" state. In addition, when the cross-correlation time τ is small, the increase of the additive noise intensity B leads to a switch of the process from "off"→"on". Simultaneously, the increase of the cross-correlation intensity λ of CCSW noises contributes to maintaining the current state. When the cross-correlation time is large, the high concentration state has two peaks and the stationary probability distribution presents a three-peak structure.

Keywords: bistable system; cross-correlated sine-Wiener noises; switch process; three-peak structure; stationary probability distribution; mean first passage time

1. Introduction

Biological systems are permeated with deterministic laws and randomness. Noise are inevitable at every level of biology, from the most essential molecular, sub-cellular processes to the kinetics of tissues, organs, organisms and populations [1]. According to different origination of noise, noise can be divided into two terms: intrinsic and extrinsic noise [2–5]. Intrinsic noise originates from the stochasticity of biochemical events, while extrinsic noise is caused by status differences in individual

cells, e.g., ribosomes and metabolites, the concentration of RNA polymerases or local environmental conditions [6]. Some experimental and theoretical studies have shown that noise may lead to genetic diseases, gene damage, etc. [7,8]. However, over the past few decades, it has been revealed that noise may also play a positive role in various dynamic systems and dynamic processes [9,10], for example, stochastic transitions [11] and switch processes [3,12].

Experimental studies have exposed that fluctuations occur in various stages of gene expression, including transcription, degradation, translation, binding, and so on [6,13,14] and noise affects gene expression [15]. Smolen et al. [16] proposed a simple model of gene transcription system dynamics, which is a bistable model with a positive feedback loop. They pointed out that the simple model manifested multiple stable state and brief perturbations could switch the model between those states. Based on this model, Liu et al. showed that the switch process could be successfully induced by the fluctuation of the rate of degradation and the synthesis of transcription factors [17]. The state transition of a rapid response to environmental changes is a common and important phenomenon in biological systems. Noise can also be used to regulate the dynamics of bistable genetic regulatory systems [18]. Wang et al. [19] further considered the effect of a time delay on the switch process. The related studies have focused on white Gaussian noise and colored noise [3,17,19–24]. However, the range of the Gaussian noise is unbounded and large values can be obtained, but the nature of real physical quantities is always bounded. The use of Gaussian noise may lead to unreasonable results in some cases [25,26]. Therefore, researchers have explored the modelling of bounded noise in dynamic systems [27]. Among them, sine-Wiener noise is the most widely used form of bounded noise [28] that is generated by a sinusoidal function with a constant amplitude, constant frequency and random change of phase with the Wiener process. Sinusoidal functions are bounded, resulting in their noise values not exceeding a fixed amplitude. In recent years, the influence of cross-correlated sine-Wiener (CCSW) noises on nonlinear dynamic systems has attracted wide attention [29,30]. Furthermore, our previous studies [31–34] revealed temporal coherent resonance phenomenon induced by CCSW noises in regular and small-world neuronal networks and indicated the occurrence of CCSW noise-induced coherent resonance. The increasing degree of correlation of CCSW noises may enhance or impair temporal regularity, which is dependent on the cross-correlation time [34]. CCSW noises in the gene transcriptional regulatory system has not been reported to date. Therefore, this study focuses on the influence of CCSW noises on the switch process in the gene transcriptional regulatory system.

2. Model and algorithm

Smolen et al. [16] have developed a simple kinetic model to examine the complex dynamic activity of genetic regulatory systems. The dynamics of the system are governed by a single ordinary differential equation to determine the concentration of the transcription factor activator (TF-A):

$$\frac{dx}{dt} = \frac{k_f x^2}{x^2 + K_d} - k_d x + R_{bas} \quad , \tag{1}$$

where $x(t)$ denotes the concentration of TF-A. k_d and R_{bas} represent the decomposition rate and basic synthesis rate of TF-A, respectively. K_d describes the dissociation concentration of the TF-A dimer from the responsive elements, TF-Res. Under the following parameters:

$$\left[-\left(\frac{k_f+R_{bas}}{3k_d}\right)^3+\frac{K_d\left(k_f+R_{bas}\right)}{6k_d}-\frac{K_dR_{bas}}{2k_d}\right]^2+\left[\frac{K_d}{3}-\left(\frac{k_f+R_{bas}}{3k_d}\right)^2\right]^3<0\ , \tag{2}$$

the potential

$$U_0(x)=k_f\sqrt{K_d}\arctan\frac{x}{\sqrt{K_d}}+\frac{k_d}{2}x^2-(R_{bas}+k_f)x\ . \tag{3}$$

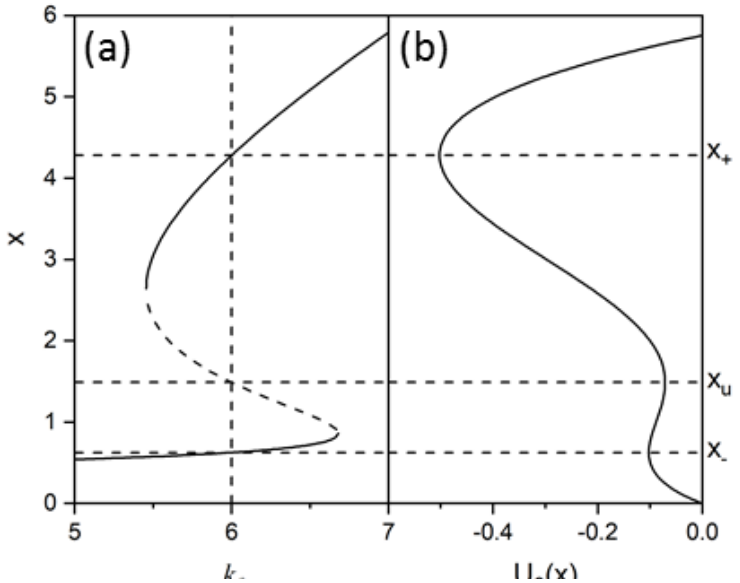

Figure 1. (a) Bifurcation plot for the steady state of TF-A on the control parameter of the transcription rate k_f. (b) The bistable potential of Eq (3). k_f = 6, K_d = 10, k_d = 1, and R_{bas} = 0.4.

Figure 1(a) shows that when K_d = 10, k_d = 1, R_{bas} = 0.4, and k_f is in the interval [5.45, 6.68], each value of k_f corresponds to three TF-A, representing two steady states and one unstable state. The corresponding bistable potential U_0 is shown in Figure 1b. When k_f = 6, the stable steady states are $x_-\approx 0.62685$ and $x_+\approx 4.28343$ and the unstable steady state is $x_u\approx 1.48971$, as shown in Figure 1. To simulate the stochastic effects of the biochemical reaction rates R_{bas} and k_d, it is assumed that the stochasticity is added to the reaction rates as $k_d\rightarrow k_d+\eta_1(t)$ and $R_{bas}\rightarrow R_{bas}+\eta_2(t)$. Here, multiplicative and additive cross-correlated sine-Wiener noises $\eta_1(t)$ and $\eta_2(t)$ are introduced into the original deterministic kinetics. Thus,

$$\frac{dx}{dt}=\frac{k_fx^2}{x^2+K_d}-\left[k_d+\eta_1(t)\right]x+R_{bas}+\eta_2(t)\,. \tag{4}$$

The explicit definitions of CCSW noises are represented as follows:

$$\eta_1(t)=A\sin\left(\sqrt{\frac{2}{\tau_1}}\omega_1(t)\right), \tag{5}$$

$$\eta_2(t) = B\sin\left(\sqrt{\frac{2}{\tau_2}}\omega_2(t)\right). \tag{6}$$

The noise strength and self-correlation times of η_1(t) and η_2(t) are indicated as A, B, τ_1 and τ_2. ω_1 and ω_2 are two cross-correlated standard Wiener processes, i.e., $\langle\omega_1(t)\omega_2(t')\rangle = \langle\omega_1(t')\omega_2(t)\rangle = \lambda\cdot\min(t,t')$. $\langle\cdots\rangle$ denotes an ensemble average and $\min(t,t')$ denotes taking the smaller value between t and t'. As previously mentioned, the statistical properties of $\eta_1(t)$ and $\eta_2(t)$ are given by:

$$\langle\eta_1(t)\rangle = \langle\eta_2(t)\rangle = 0 \ , \tag{7}$$

$$\langle\eta_1(t)\eta_1(t')\rangle = \frac{A^2}{2}\exp\left(-\frac{t-t'}{\tau_1}\right)\left[1-\exp\left(-\frac{4t'}{\tau_1}\right)\right] \ , \tag{8}$$

$$\langle\eta_2(t)\eta_2(t')\rangle = \frac{B^2}{2}\exp\left(-\frac{t-t'}{\tau_2}\right)\left[1-\exp\left(-\frac{4t'}{\tau_2}\right)\right], \tag{9}$$

$$\langle\eta_1(t)\eta_2(t')\rangle = \langle\eta_1(t')\eta_2(t)\rangle = \lambda\frac{AB}{2}\exp\left(-\frac{t-t'}{\tau}\right)\left[1-\exp\left(-\frac{4t'}{\tau}\right)\right], t>t', \tau_1=\tau_2=\tau \ . \tag{10}$$

Here, λ and τ stand for the cross-correlation intensity ($0 \le \lambda \le 1$) and cross-correlation time between η_1(t) and η_2(t), respectively. The coupling between CCSW noises results in a difficulty of directly integrating the dynamic equation (4). However, CCSW noises can be decoupled and transformed as below [32,35,36]:

$$\xi_1(t) = A\sin\left(\sqrt{\frac{2}{\tau}}\omega_\alpha(t)\right), \tag{11}$$

$$\xi_2(t) = B\lambda\sin\left(\sqrt{\frac{2}{\tau}}\omega_\alpha(t)\right) + B\sqrt{1-\lambda^2}\sin\left(\sqrt{\frac{2}{\tau}}\omega_\beta(t)\right). \tag{12}$$

Here, ω_α and ω_β denote two independent standard Wiener processes. Note that the transformations do not change the statistical properties of Eqs 7–10. After the above-mentioned decoupling operations, the dynamic equation (4) is rewritten as follows:

$$\frac{dx}{dt} = \frac{k_f x^2}{x^2+K_d} - \left[k_d+\xi_1(t)\right]x + R_{bas} + \xi_2(t). \tag{13}$$

According to the Euler forward procedure, Eq (13) is discretized in our numerical simulations as follows [37]:

$$
\begin{aligned}
x\left(t+\Delta t\right) &= x\left(t\right)+\left[\frac{k_f x^2}{x^2+K_d}-k_d x+R_{bas}\right]\Delta t \\
&-Ax\left(t\right)X_1\left(t\right)\Delta t+B\left[\lambda X_1\left(t\right)+\sqrt{1-\lambda^2}X_2\left(t\right)\right]\Delta t \\
&-\frac{1}{2}AX_1\left(t\right)\left\{-Ax\left(t\right)X_1\left(t\right)+B\left[\lambda X_1\left(t\right)+\sqrt{1-\lambda^2}X_2\left(t\right)\right]\right\}\Delta t^2,
\end{aligned}
\tag{14}
$$

with

$$X_1(t)=\sin\left(\sqrt{2/\tau}\,\omega_\alpha(t)\right), \tag{15}$$

$$X_2(t)=\sin\left(\sqrt{2/\tau}\,\omega_\beta(t)\right), \tag{16}$$

$$\omega_\alpha(t)=\omega_\alpha(t-\Delta t)+\sqrt{-2\Delta t\ln\chi_1}\cos\left(2\pi\chi_2\right), \tag{17}$$

$$\omega_\beta(t)=\omega_\beta(t-\Delta t)+\sqrt{-2\Delta t\ln\chi_3}\cos\left(2\pi\chi_4\right). \tag{18}$$

Here, χ_1, χ_2, χ_3 and χ_4 are four independent random numbers uniformly distributed on the unit interval. $\Delta t = 0.001$ is the time step.

3. Results and discussion

3.1. Steady state characteristics

We first investigated the effect of the cross-correlation time τ on the steady-state probability distribution (SPD) and switching process. For a given time series of a concentration of TF-A, the total number of time points is N. The observed number n_i of x within the distance bin from x_i to $x_i + \triangle x$ is counted for a long x (t) sequence that discards transient processing, $0 < x < 10$, $\triangle x = 0.1$. The probability n_i/N of each distance is calculated, and thus, the steady-state probability distribution (SPD) is obtained. As shown in Figure 2, the novel phenomenon is that the high concentration state of SPD undergoes a transition from unimodal to bimodal, and therefore, the overall SPD has a three-peak structure with a larger noise cross-correlation time τ. With the increase of the noise cross-correlation time τ, the peak of the probability distribution in the low steady state increases, which corresponds to a decrease of the TF-A monomer concentration and the occurrence of a switch process (i.e., "on"→"off"). That is, the cross-correlation time τ not only causes the on-off switching process but also leads to the formation of double peaks of a high steady state and a triple peaks structure in the overall SPD. Tristability itself may be valuable; for example, a genetic tristate can be found or used in various biochemical networks. This triple peaks structure has only ever been observed in an experiment in synthetic biology by Rui Ma et al. [38]. They noted that the triple steady state phenomenon resulted from the discrete and fluctuating nature of a small system. Stem cells and other kinds of multipotent cells might differentiate into two states, and then, one of them redifferentiates into three states according to Waddington's epigenetic landscape [39]. Our work also provides a possible mechanism for the formation of the triple peaks structure.

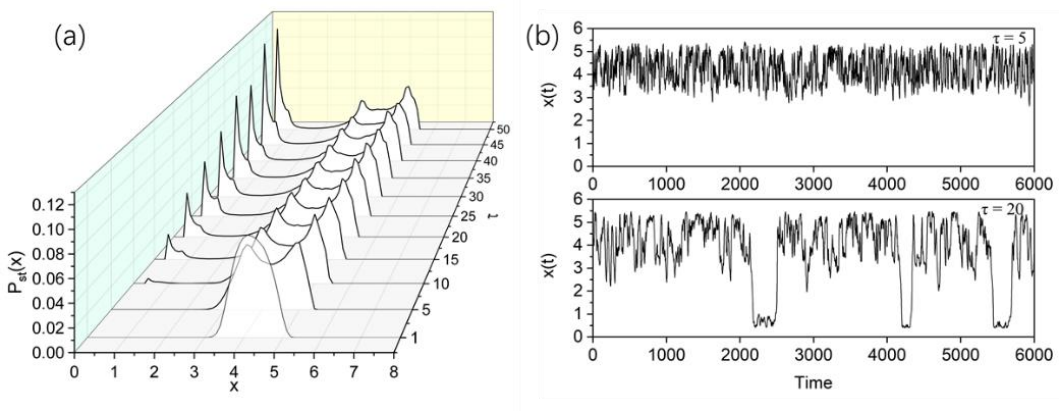

Figure 2. (a) Probability distribution of $x(t)$ for different cross-correlation time τ with $A = 0.1$, $B = 0.1$ and $\lambda = 0.5$. (b). Sample paths of $x(t)$ with $\tau = 0.5$ and $\tau = 20$. The other parameter values are the same as those in Figure 1.

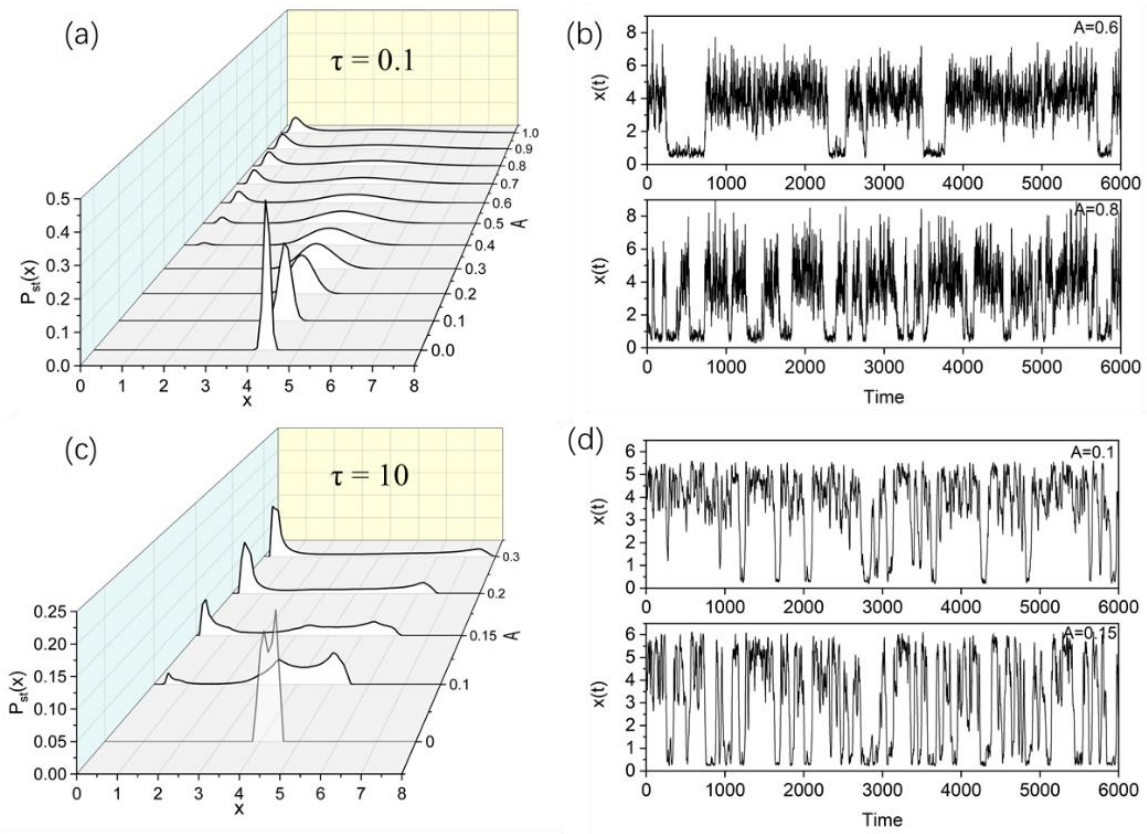

Figure 3. Probability distribution and sample paths of $x(t)$ for different multiplicative noise intensities A. The additive noise intensity $B = 0.2$, the cross-correlation intensity $\lambda = 0.3$, the cross-correlation intensity $\tau = 0.1$ and $\tau = 20$. The other parameter values are the same as those in Figure 1.

Based on the different effects of the noise cross-correlation time τ on the system, the influence of the other parameters of noise is considered when different values of the cross-correlation time τ are selected. First, we consider the effect of multiplicative noise, which is shown in Figure 3. It can be seen that the increase of the multiplicative noise intensity A leads the system to be in a low steady state, corresponding to the decrease of the TF-A monomer concentration and the switch to an off position when τ is smaller and larger. However, multiplicative noise has a strong influence on the bimodal structure of a high steady state. With the increase of the multiplicative noise intensity A, the distance between the two peaks increases. Finally, the left peak of the two peaks weakens and disappears, and the whole peak structure returns to the double peak structure. The extreme value of the peak of the high steady state deviates from the steady-state point to the right.

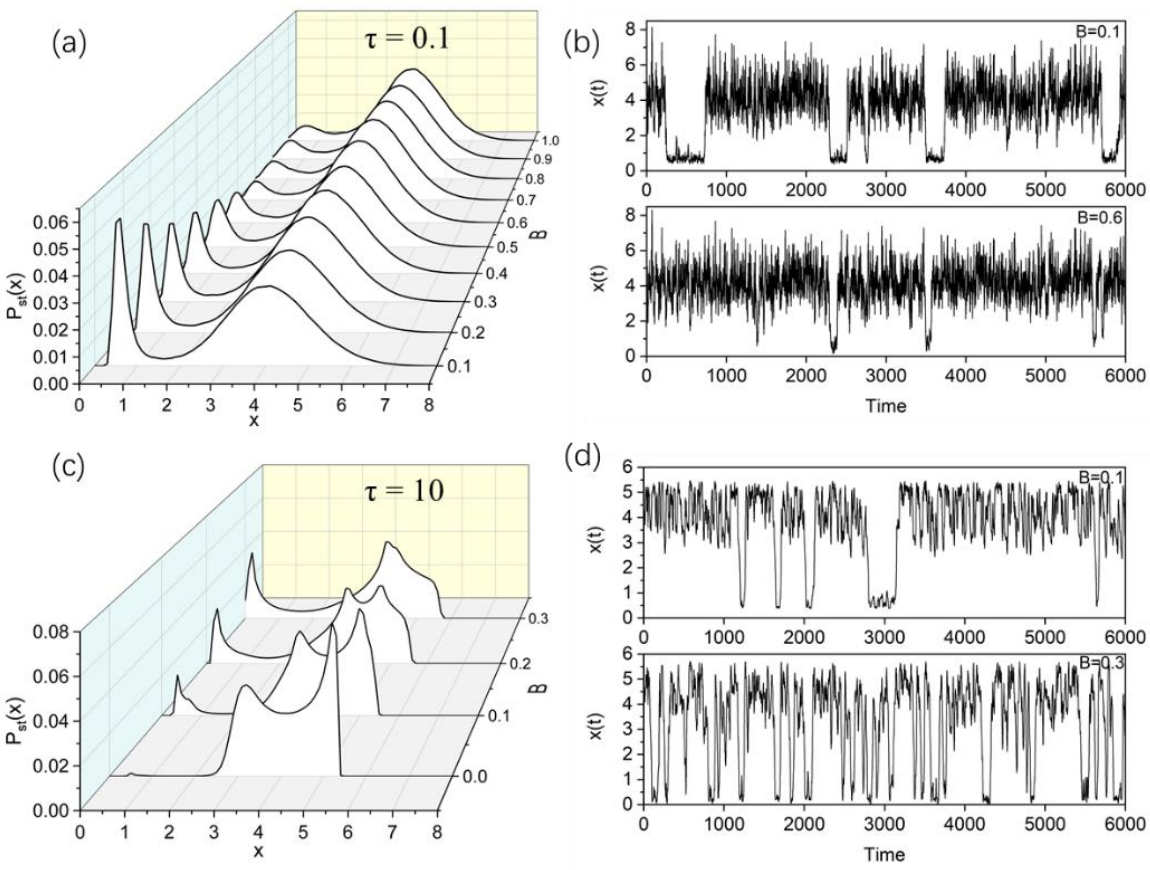

Figure 4. Probability distribution and sample paths of $x(t)$ for different additive noise intensities B. (a-b) The multiplicative noise intensity A = 0.6, the cross-correlation intensity λ = 0.1, the cross-correlation intensity τ = 0.1. (c-d) the additive noise intensity A = 0.1, the cross-correlation intensity λ = 0.3, the cross-correlation intensity τ = 20. The other parameter values are the same as those in Figure 1.

Then, we investigated the effect of additive noise, which is shown in Figure 4. When τ is small, the increase of the additive noise intensity B leads to a decrease of the low concentration and an increase of the high concentration (Figure 4a). Correspondingly, the time series diagrams

of the TF-A monomer concentrations for additive noise intensities $B = 0.1$ and $B = 0.6$ are given in Figure 4b. It can be seen that the increase of the additive noise intensity B drives the system to the high steady state, which corresponds to an increase of the TF-A monomer concentration, and the system switches to the "on" position. However, when τ is large, the distance between the two peaks decreases, and they become a single peak with the increase of additive noise B, as shown in Figure 4c–d. At the same time, switching of the process from "on" to "off" is induced.

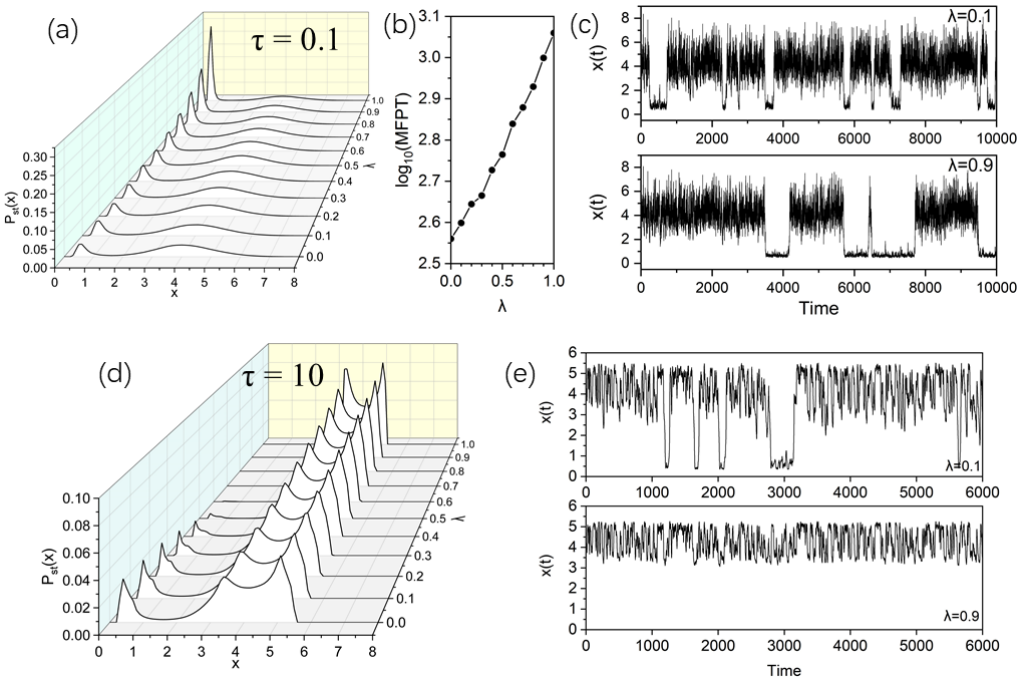

Figure 5. (a, d) Probability distribution, (b) MFPT and (c, e) sample paths of $x(t)$ for different cross-correlation intensities λ. (a) $A = 0.6$, $B = 0.2$, $\tau = 0.1$. (d) $A = 0.1$, $B = 0.1$ and $\tau = 10$. The other parameter values are the same as those in Figure 1.

Figure 5a shows the effect of the cross-correlation intensity on SPD when τ is small. It can be found that an increase of the noise cross-correlation intensity λ causes the SPD to shift from a high steady state to a low concentration state. However, it is interesting to note that the shift between the different concentration states does not mean the process switches from "on" → "off". As can be seen from Figure 5b, the mean first passage time (MFPT), which is the mean time spent in one state before switching to another, monotonously increases with the increase of the cross-correlation intensity λ. The mean first passage time reflects the switching time between on and off states. That is, the smaller MFPT is, the more frequent the jump between the two steady states. On the contrary, the longer MFPT is, the longer the system maintains the current state. The corresponding time series of the TF-A monomer concentration, as shown in Figure 5c, indicates that a large cross-correlation intensity λ can maintain the TF-A monomer in the current concentration state, that is, keep in the "on" or "off" state. When τ is large, the increase of the cross-correlation intensity λ makes the high-concentration binary states more distinct (Figure 5d–e) and also causes the process to switch

from “off” to “on”. Contrary to the case of a smaller τ, for a large cross-correlation intensity λ, the system cannot maintain the current state when τ is larger.

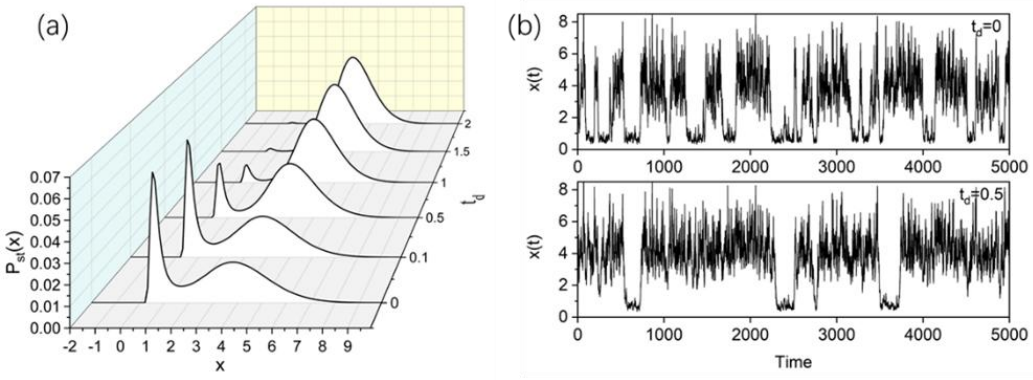

Figure 6. Probability distribution and sample paths of $x(t)$ for different delay times t_d. $A = 0.8$, $B = 0.1$, $\lambda = 0.5$ and $\tau = 0.1$. The other parameter values are the same as those in Figure 1.

In addition, there is feedback delay in the real system, so equation (1) becomes:

$$\frac{dx(t)}{dt} = \frac{k_f x(t-t_d)^2}{x(t-t_d)^2 + K_d} - \left[k_d + \eta_1(t)\right]x(t) + R_{bas} + \eta_2(t), \tag{19}$$

t_d is the delay time, and the other parameters are the same as in Eq (1).

Figure 6 shows that the feedback time delay plays an important role in random systems. With the increase of the delay time, the peak of the probability distribution at a low steady state decreases, while those of the high steady state increase, corresponding to an increase of the TF-A monomer concentration, and the system switches from “off” to “on”.

3.2. Mean first passage time (MFPT)

When the system is stochastic bistable, the quantity of interest is the time from one state to another. This time is a random variable, often referred to as the first passage time. Here, we consider the mean first passage time (MFPT) [40]. We record the time of the process $x(t)$ to reach the low concentration state x_- from the initial condition $x\ (t = 0) = x_+$ (the high concentration state) for the first time and repeat the process 1000 times to obtain the mean first pass time (MFPT). The MFPT can quantify the effect of noise on the transition between two steady states. The main results are shown in Figures 7–10.

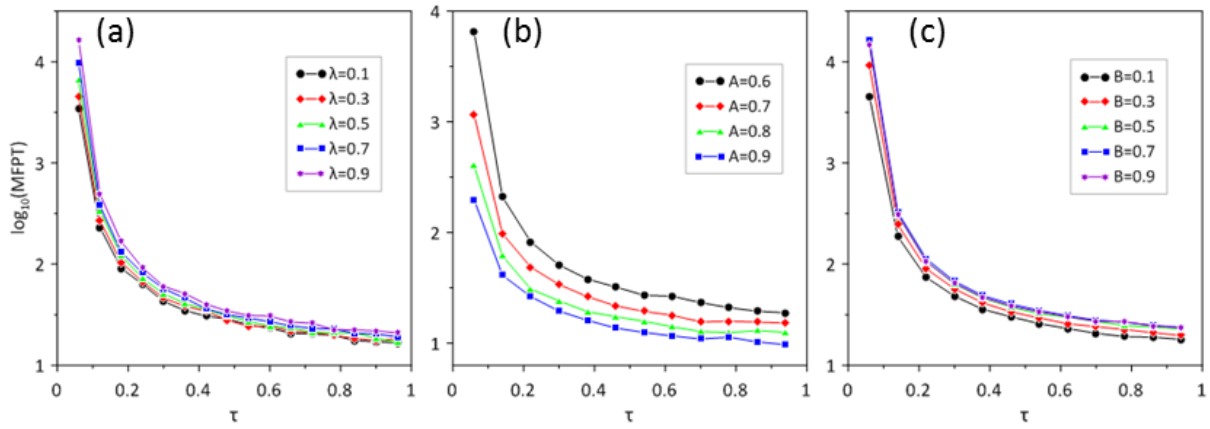

Figure 7. The MFPT as a function of the cross-correlation τ (a) for different cross-correlation intensities, λ = 0.1, 0.3, 0.5, 0.7, 0.9 with A = 0.6, B = 0.2; (b) for different multiplicative noise intensities, A = 0.6, 0.7, 0.8, 0.9 with B = 0.2, λ = 0.5; (c) for different additive noise intensities, B = 0.1, 0.3, 0.5, 0.7, 0.9 with A = 0.6, λ = 0.5.

The MFPT as a function of the cross-correlation time τ for different cross-correlation intensities λ, multiplicative noise intensities A and additive noise intensities B is shown in Figure 7. It can be seen that the MFPT always decreases monotonously with the increase of the cross-correlation time τ. These results indicate that the switch of the process from "on" to "off" becomes easier when the cross-correlation time τ is larger. In addition, the MFPT increases with the increase of the cross-correlation intensity λ, as illustrated in Figures 7a and 10, while the MFPT decreases with the increase of the multiplicative noise intensity A, as shown in Figures 7b and 8. Then, the MFPT varies nonmonotonically with the increase of the additive noise intensity B when λ = 0.5, as shown in Figures 7c, 9 and 10a.

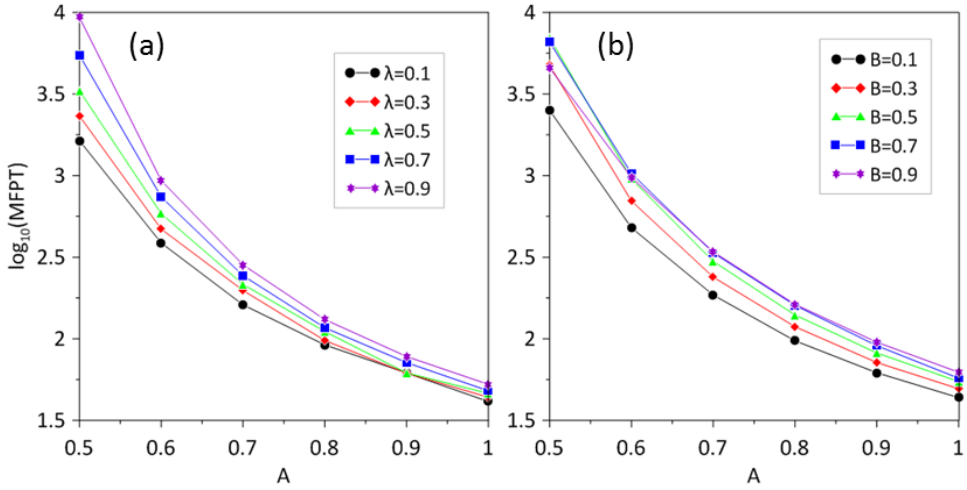

Figure 8. The MFPT as a function of the multiplicative noise intensity A. (a) for different cross-correlation intensities, λ = 0.1, 0.3, 0.5, 0.7, 0.9 with B = 0.2 and τ = 0.1; (b) for different additive noise intensities, B = 0.1, 0.3, 0.5, 0.7, 0.9 with λ = 0.5 and τ = 0.1.

Figure 8 shows the MFPT as a function of multiplicative noise A for different cross-correlation intensities λ and additive noise intensities B. The MFPT always decreases monotonously with the increase of the multiplicative noise intensity A, which is similar to the effect of the cross-correlation time τ. In addition, there are both monotonic and non-monotonic changes with the increase of λ or B when A is fixed in the MFPT as shown in Figure 8a,b. Further results are presented in Figures 9 and 10.

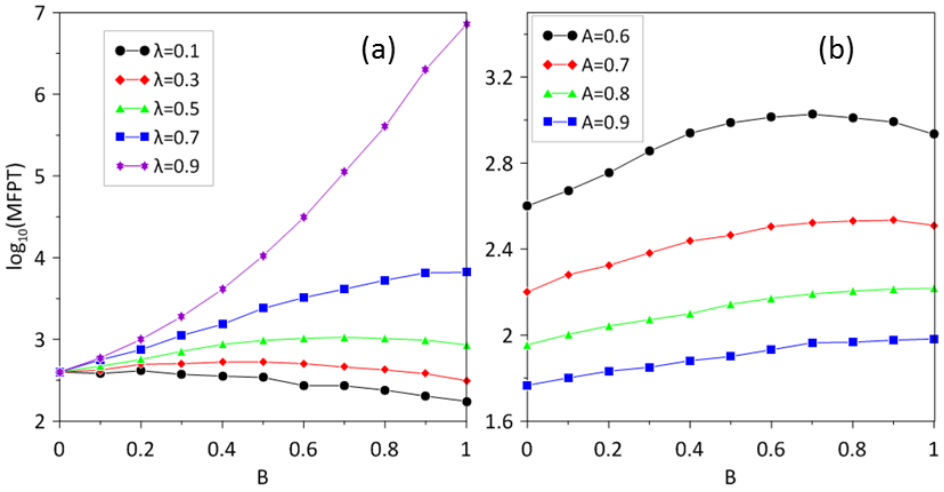

Figure 9. The MFPT as a function of the additive noise intensity B; (a) for different cross-correlation intensities, λ = 0.1, 0.3, 0.5, 0.7, 0.9 with A = 0.6 and τ = 0.1; (b) for different multiplicative noise intensities, A = 0.6, 0.7, 0.8, 0.9 with λ = 0.5 and τ = 0.1.

Then, the MFPT as a function of the additive noise intensity B for different cross-correlation intensities and multiplicative noise intensities is shown in Figure 9. The MFPT slightly decreases when the cross-correlation intensity λ is small (λ = 0.1). Moreover, the MFPT first increases and then decreases when λ reaches a moderate value (λ = 0.5). Furthermore, the MFPT increases monotonously and rapidly with a large λ (λ = 0.9). The MFPT showed different trends with the enhancement of B for different values of λ (monotonic decrease, non-monotonic, monotonic increase), which is also shown in Figure 10a. The larger λ is, the more TF-A is able to maintain its current state and the larger MFPT is (Figure 5b). Therefore, it can be inferred that the monotonous decrease of the black dotted line in Figure 9a is due to the role of B when λ is small. This result suggests that the increasing additive noise intensity B also makes the switching process easier. When the value of λ is large, the rapid increase of the MFPT is caused by the enhancement of the ability of λ to maintain the current state. Therefore, when the value of λ is set moderately, the enhancement of B reduces the MFPT, while a moderate value of λ allows the MFPT to be increased, which results in an increase and then a decrease of the MFPT. Moreover, Figure 9b shows that the above nonmonotonicity is destroyed with the increase of A when the value of λ is moderate (λ = 0.5), and the MFPT then undergoes a monotonous increase.

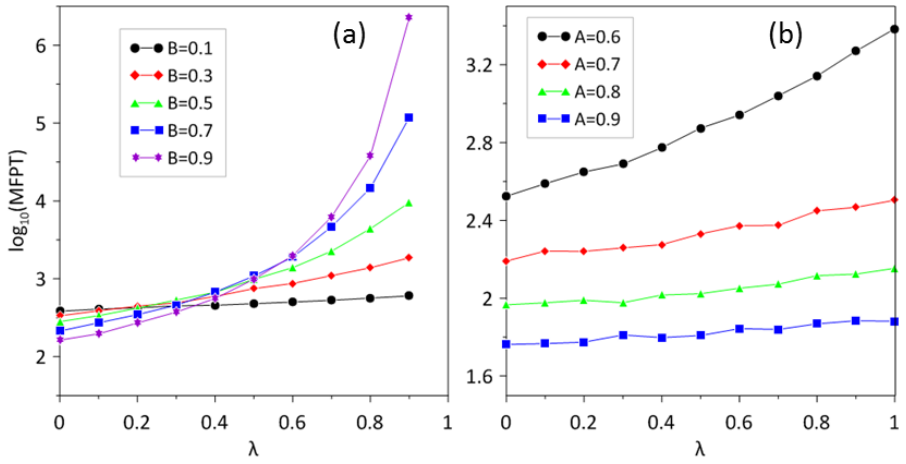

Figure 10. The MFPT as a function of the cross-correlation intensity λ; (a) for different additive noise intensities, B = 0.1, 0.3, 0.5, 0.7, 0.9 with A = 0.6 and τ = 0.1; (b) for different multiplicative noise intensities, A = 0.6, 0.7, 0.8, 0.9 with λ = 0.5 and τ = 0.1.

Figure 10 shows the MFPT as a function of the cross-correlation intensity λ for different additive noise intensities B and multiplicative noise intensities A. The MFPT always increases monotonously when an increase of the cross-correlation intensity λ occurs. The results imply that the switch of the process from "on" to "off" becomes difficult. The MFPT decreases monotonically with the increase of B in the region of $0 < \lambda < 0.1$. The MFPT increases monotonically with the increase of B in the region of $0.6 < \lambda < 1$ and presents non-monotonicity in the region of $0.1 < \lambda < 0.6$ (Figure 10a). In Figure 10b, when A increases, the trend of the MFPT increases slowly with the increase of λ. That is, the role of A is opposite to that of λ.

4. Conclusion

In this study, we investigated switch processes in a transcriptional regulatory system driven by CCSW noises. It was found that the increase of the multiplicative noise intensity A and cross-correlation time τ could reduce the concentration of the TF-A monomer and switch to an "off" state. In addition, the effect of the cross-correlation time on SPD presents a novel phenomenon. When the cross-correlation time τ is small, the enhancement of the cross-correlation intensity λ presents a seemingly contradictory result, that is, an increase of the MFPT and an increase of the low steady state, which indicates that the role of the cross-correlation intensity λ is to maintain the current state. The combined effects of the additive noise intensity B and cross-correlation intensity λ show that when λ is small, the effect of maintaining the current state is weak. The enhancement of B leads the SPD to shift from a high steady state to a low concentration one, a switch to the "on" state, and a monotonous decrease of MFPT. Next, when λ is large, the ability to maintain the current state is enhanced and the MFPT increases rapidly. Third, when λ is moderate, the enhancement of B decreases the MFPT and the increase of cross-correlation intensity λ increases the MFPT, which results in the non-monotonicity of the MFPT (first increases and then decreases).

When the cross-correlation time τ is large, the single peak of the high steady state splits into two peaks and the SPD has a three-peak structure. The effect of the cross-correlation intensity λ is different from that of the small cross-correlation time τ. The enhancement of the cross-correlation

intensity λ leads to a decrease of the low steady state and an increase of the high steady state, and the bimodal structure of the high steady state is sharper. The SPD is shifted from a high steady state to a low one when the additive noise intensity is decreased. However, the effect of multiplicative noise and additive noise is opposite to that of the double peaks in the high concentration state. The increase of the multiplicative noise intensity leads to an increase of the distance between two peaks in the high concentration state, while the increase of the intensity of additive noise presents an inverse process, that is, the distance between the two peaks decreases until they transition into a single peak. The above results show different characteristics from white Gaussian noise, which lays a foundation for further research on the influence of CCSW noises on nonlinear systems.

Acknowledgments

This work was supported by the National Natural Science Foundation of China (Grant No.11675060, 91730301, 11804111), the Huazhong Agricultural University Scientific and the Fundamental Research Funds for the Central University (Grant No. 26622018JC017).

Conflict of Interest

The authors declare that they have no competing interests.

References

1. L.S. Tsimring, Noise in biology, *Rep. Prog. Phys.*, **77**(2014), 026601.
2. Y. Harada, T. Funatsu, K. Murakami, et al., Single-molecule imaging of RNA polymerase-DNA interactions in real time, *Biophys. J.*, **76** (1999), 709–715.
3. J. Hasty, J. Pradines, M. Dolnik, et al., Noise-based switches and amplifiers for gene expression, *Proc. Natl. Acad. Sci. U. S. A.*, **97** (2000), 2075–2080.
4. P. S. Swain, M. B. Elowitz and E. D. Siggia, Intrinsic and extrinsic contributions to stochasticity in gene expression, *Proc. Natl. Acad. Sci. U. S. A.*, **99** (2002), 12795–12800.
5. C. V. Rao, D. M. Wolf and A. P. Arkin, Control, exploitation and tolerance of intracellular noise, *Nature*, **420** (2002), 231–237.
6. L. Bandiera, A. Pasini, L. Pasotti, et al., Experimental measurements and mathematical modeling of biological noise arising from transcriptional and translational regulation of basic synthetic gene circuits, *J. Theor. Biol.*, **395** (2016), 153–160.
7. S. Rulands and B. D. Simons, Tracing cellular dynamics in tissue development, maintenance and disease, *Curr. Opin. Cell Biol.*, **43** (2016), 38–45.
8. M. A. Nowak and B. Waclaw, Genes, environment, and "bad luck", *Science*, **355** (2017), 1266–1267.
9. L. Gammaitoni, P. Hänggi, P. Jung, et al., Stochastic resonance, *Rev. Mod. Phys.*, **70** (1998), 223–287.
10. A. S. Pikovsky and J. Kurths, Coherence resonance in a noise-driven excitable system, *Phys. Rev. Lett.*, **78** (1997), 775–778.
11. C. Van den Broeck, J. M. Parrondo, and R. Toral, Noise-induced nonequilibrium phase transition, *Phys. Rev. Lett.*, **73** (1994), 3395–3398.

12. J. Hasty, F. Isaacs, M. Dolnik, et al., Designer gene networks: Towards fundamental cellular control, *Chaos,* **11** (2001), 207–220.
13. H. Chen, K. Shiroguchi, H. Ge, et al., Genome-wide study of mRNA degradation and transcript elongation in Escherichia coli, *Mol. Syst. Biol.,* **11** (2015), 781.
14. G. W. Li and X. S. Xie, Central dogma at the single-molecule level in living cells, *Nature,* **475** (2011), 308–315.
15. A. Sanchez, S. Choubey and J. Kondev, Regulation of noise in gene expression, *Annu. Rev. Biophys.,* **42** (2013), 469–491.
16. P. Smolen, D. A. Baxter and J. H. Byrne, Frequency selectivity, multistability, and oscillations emerge from models of genetic regulatory systems, *Am. J. Physiol.*, **274** (1998), 531–542.
17. Q. Liu and Y. Jia, Fluctuations-induced switch in the gene transcriptional regulatory system, *Phys. Rev. E Stat. Nonlin. Soft Matter Phys.,* **70** (2004), 041907.
18. Y. Sharma, P. S. Dutta and A. K. Gupta, Anticipating regime shifts in gene expression: The case of an autoactivating positive feedback loop, *Phys. Rev. E Stat. Nonlin. Soft Matter Phys.,* **93** (2016), 032404.
19. C. Wang, M. Yi, K. Yang, et al., Time delay induced transition of gene switch and stochastic resonance in a genetic transcriptional regulatory model, *BMC Syst. Biol.,* **6** (2012), S9.
20. C. J. Wang and K. L. Yang, Correlated noise-based switches and stochastic resonance in a bistable genetic regulation system, *Eur. Phys. J. B,* **89** (2016), 173.
21. X. Chen, Y. M. Kang and Y. X. Fu, Switches in a genetic regulatory system under multiplicative non-Gaussian noise, *J. Theor. Biol.,* **435** (2017), 134–144.
22. C. Zhang, L. P. Du, Q. S. Xie, et al., Emergent bimodality and switch induced by time delays and noises in a synthetic gene circuit, *Physica A,* **484** (2017), 253–266.
23. X. Fang, Q. Liu, C. Bohrer, et al., Cell fate potentials and switching kinetics uncovered in a classic bistable genetic switch, *Nat. Commun.,* **9** (2018), 2787.
24. C. Li, Z. L. Jia and D. C. Mei, Effects of correlation time between noises on the noise enhanced stability phenomenon in an asymmetric bistable system, *Front. Phys.,* **10** (2015), 95–101.
25. A. d'Onofrio and A. Gandolfi, Resistance to antitumor chemotherapy due to bounded-noise-induced transitions, *Phys. Rev. E Stat. Nonlin. Soft Matter Phys.,* **82** (2010), 061901.
26. A. d'Onofrio, Bounded-noise-induced transitions in a tumor-immune system interplay, *Phys. Rev. E Stat. Nonlin. Soft Matter Phys.,* **81** (2010), 021923.
27. A. D'Onofrio, Bounded noises in physics, biology, and engineering, Birkhäuser Basel, 2013.
28. G.Q. Cai and C. Wu, Modeling of bounded stochastic processes, *Probabilist. Eng. Mech.,* **19** (2004), 197–203.
29. C.-J. Wang, Q.-F. Lin, Y.-G. Yao, et al., Dynamics of a stochastic system driven by cross-correlated sine-Wiener bounded noises, *Nonlinear Dyn.,* **95** (2018), 1941–1956.
30. W. Guo and D.-C. Mei, Stochastic resonance in a tumor–immune system subject to bounded noises and time delay, *Physica A,* **416** (2014), 90–98.
31. Y. G. Yao, W. Cao, Q. M. Pei, et al., Breakup of Spiral Wave and Order-Disorder Spatial Pattern Transition Induced by Spatially Uniform Cross-Correlated Sine-Wiener Noises in a Regular Network of Hodgkin-Huxley Neurons, *Complexity,* **2018** (2018), 1–10.
32. Y. Yao, C. Ma, C. Wang, et al., Detection of sub-threshold periodic signal by multiplicative and additive cross-correlated sine-Wiener noises in the FitzHugh–Nagumo neuron, *Physica A,* **492** (2018), 1247–1256.

33. Y. Yao, M. Yi and D. Hou, Coherence resonance induced by cross-correlated sine-Wiener noises in the FitzHugh–Nagumo neurons, *Int. J. Mod. Phys. B,* **31** (2017), 1750204.
34. G. H. Cheng, R. Gui, Y. G. Yao, et al., Enhancement of temporal regularity and degradation of spatial synchronization induced by cross-correlated sine-Wiener noises in regular and small-world neuronal networks, *Physica A,* **520** (2019), 361–369.
35. W. Guo, L.-C. Du and D.-C. Mei, Transitions induced by time delays and cross-correlated sine-Wiener noises in a tumor–immune system interplay, *Physica A,* **391** (2012), 1270–1280.
36. S. Q. Zhu, Steady-State Analysis of a Single-Mode Laser with Correlations Between Additive and Multiplicative Noise, *Phys. Rev. A,* **47** (1993), 2405–2408.
37. P. Liu and L. J. Ning, Transitions induced by cross-correlated bounded noises and time delay in a genotype selection model, *Physica A,* **441** (2016), 32–39.
38. R. Ma, J. Wang, Z. Hou, et al., Small-number effects: a third stable state in a genetic bistable toggle switch, *Phys. Rev. Lett.,* **109** (2012), 248107.
39. J. E. Ferrell, Jr., Bistability, bifurcations, and Waddington's epigenetic landscape, *Curr Biol,* **22** (2012), R458–R466.
40. Y. Jia and J. R. Li, Transient properties of a bistable kinetic model with correlations between additive and multiplicative noises: Mean first-passage time, *Phys. Rev. E Stat. Nonlin. Soft Matter Phys.,* **53** (1996), 5764–5768.

AIMS Press